Hindawi
Mathematical Problems in Engineering
Volume 2020, Article ID 8382734, 10 pages
https://doi.org/10.1155/2020/8382734

Research Article

Adaptive Cruise Control Strategy Design with Optimized Active Braking Control Algorithm

Wenguang Wu,[1,2] **Debiao Zou**,[3] **Jian Ou**,[1] **and Lin Hu**[1,2]

[1]*School of Automotive & Mechanical Engineering, Changsha University of Science & Technology, Changsha 410114, China*
[2]*Hunan Key Laboratory of Smart Roadway and Cooperative Vehicle-Infrastructure Systems, Changsha 410114, China*
[3]*Mechanical and Vehicle Engineering, Hunan University, Changsha 410006, China*

Correspondence should be addressed to Lin Hu; hulin@csust.edu.cn

Received 8 June 2020; Accepted 26 June 2020; Published 21 July 2020

Guest Editor: Yong Chen

The braking quality is considered as the most important performance of the adaptive control system that influences the vehicle safety and ride comfort remarkably. This research is aimed at designing an adaptive cruise control (ACC) system based on active braking algorithm using hierarchical control. Taking into account the vehicle with safety and comfort, the upper decision-making controller is designed based on model predictive control algorithm. Throttle controller and braking controller are designed with feedforward and feedback algorithms as the bottom controller, where the braking controller is designed based on the hydraulic braking model. The whole model is simulated collaboratively with Amesim, Carsim, and Simulink. By comparison with the full deceleration model, the results show that the proposed algorithm can not only make the vehicle maintain a safe distance under the premise of following the target vehicle ahead effectively but also provide favorable driving comfort.

1. Introduction

In recent years, one of the most important goals in the automotive industry has been to offer passengers the highest level of safety, comfort, and efficiency by partially or completely removing driving duties from humans. Advanced Driver Assistant System (ADAS) has become a research hotspot in the field of intelligent transportation; it not only improves the road capacity [1], but also ensures the safety of drivers and vulnerable road users to some extent [2, 3]. Studies have shown that the active safety systems, such as adaptive cruise control, electronic stability control, or lane keeping assistant, which are already on the automotive market, can improve safety by decreasing the number of traffic accidents, among which the ACC helps a lot to reduce the driver's work intensity; an ACC equipped vehicle uses radar or other sensors that detect the distance and speed to other preceding vehicles (downstream vehicles) on the highway. In the absence of preceding vehicles, the ACC vehicle travels at a driver-set speed. If a preceding vehicle is detected on the highway by the vehicle's radar, the ACC system determines to control the throttle and braking system so as to maintain an expected distance and acceleration from the preceding vehicle [4].

The planning and decision-making modules are the "brain" of the vehicle and have a high degree of intelligence. All response actions of the vehicle are performed according to the instructions issued by the module. By processing and calculating the real-time state information and environmental information of the vehicle, this module can plan the most reasonable vehicle movement state and send it to the execution control module [5]. The most critical parts for the ACC, the planning and decision-making module, need to decide the optimal control target according to the relative motion state between the host vehicle and the target vehicle: expected longitudinal acceleration or distance [6]. So far, the decision algorithms of the ACC mainly have the following forms: PID feedback control, model predictive control, fuzzy logic control, and optimal control [7–10].

Longitudinal control is the basic function of ACC system where the control technology is used to achieve constant

speed driving of the vehicle, maintaining the distance between vehicles or the time between vehicles to follow the leading vehicle, identifying and tracking the curve of the vehicle ahead, automatic braking, and other functions. The quality of the longitudinal control effect has a direct impact on the safety and comfort of ACC system. The executive control module mainly achieves rapid response to the instructions issued by the planning and decision module and precise tracking of the expected goal through the precise control of the driving system and the braking system. ACC system in accordance with the working conditions can be divided into cruise mode, following mode, and overtaking mode [11]; the research scope of this article is car-following model, whose function is to keep an appropriate distance and speed with the leading vehicle. In order to further improve the effect of vehicle longitudinal control, dynamic model has become one of the key links in the field of vehicle longitudinal control. Among them, Zhan established a longitudinal dynamic model and braking system model for ACC system [12]. The researchers adopted longitudinal control method based on vehicle longitudinal inverse model and used vehicle inverse model to control electronic throttle and braking pressure [13, 14].

With the development of ACC system, more and more working conditions involve speeds of 30 km/h and below, so the vehicle longitudinal control has experienced the development process from single throttle control to combined throttle-braking control [15]. Due to strong robustness, low accuracy requirements for controlled objects, and no need for accurate modeling, classical control methods represented by PID control and numerical look-up tables are widely used. In addition, many researchers use the modified form of PID controller to study longitudinal control of vehicles, and try to improve longitudinal control effect by improving PID controller [16, 17].

Adaptive Neural Network scheme has been used in a platoon, in order to solve the traffic stability problem [18]. PID algorithm is used to directly control the accelerator pedal and the brake pedal to control the acceleration and deceleration of the vehicle to maintain the distance from the preceding vehicle [19, 20]. The fuzzy logic-based ACC controller is used to make one vehicle follow another vehicle stably, having no shock during the process of the accelerator and brake switching [21, 22]. The fuzzy ACC system with speed sign detection capability and synovial control is used for adaptive control system [23, 24]. The change of signal light is also considered to control the driving of vehicles at intersections [25]. The prospective velocity of the preceding vehicle is estimated by a prediction model based on the measured intervehicle distance and the I2V communication to enable an anticipatory driving behavior for the controlled vehicle [26].

One can conclude from the research that the previous active braking functions of adaptive cruise-following system also did not fully consider the ride comfort and hydraulic hysteresis problem. This research is aimed at designing an ACC considering the vehicle ride and proposing an analysis model based on active braking algorithm using hierarchical control.

In this paper, considering the safety, comfort, and the physical characteristics of hydraulic braking system, by switching on and off the valve and motor start-stop, adjusting the hydraulic cylinder pressure, a new ACC control strategy based on active braking is proposed. By comparison with the full deceleration model, the proposed method can improve the braking ride comfort obviously. The remainder of this paper is structured as follows: Section 2, modeling; Section 3, control algorithm research; Section 4, simulation and discussion; Section 5, conclusions.

2. Modeling

This paper is aimed at designing a control scheme that could guarantee safety considering the vehicle characteristic and ensure braking comfort at all times. As shown in Figure 1, the vehicle longitudinal dynamics model, the hydraulic braking system, and the control mechanism are included in the proposed research model. The main idea of the controller model is as follows:

(1) The real-time safety distance according to the vehicle speed and the actual distance and relative speed between leader vehicle and follower vehicle are obtained as the controller input.

(2) The limitation of the acceleration and relative distance of the follower vehicle is calculated by the longitudinal dynamics model.

(3) The expected acceleration of the follower vehicle is calculated and the optimized brake pressure is transmitted to the executive agency including active brake controller and active throttle controller.

(4) The braking pressure is produced by the hydraulic braking system, and the vehicle speed slows down. In this process, the brake pressure information is also transmitted to the longitudinal dynamics model.

2.1. Vehicle Dynamics Model. In this paper, Carsim software is used to build vehicle dynamics model for collaborative simulation. The vehicles are four-wheel drive B-class hatchback with the engine power of 125 kW, and with the hydraulic ABS braking system. The vehicle model includes 7 subsystems: the body, aerodynamics input, transmission system, braking system, steering system, suspension system, and the tire. The parameters of the vehicles are shown in Table 1. The output of the model includes the longitudinal velocity v, acceleration a, engine speed ω_e, and position S.

2.2. Vehicle Reverse Longitudinal Dynamics Model. In the ACC system, the control command from the host controller is a desired vehicle acceleration that needs to be shifted to the desired throttle opening and brake pressure by the vehicle reverse longitudinal dynamic model, which then transmitted to the vehicle longitudinal dynamics model to control the vehicle acceleration, deceleration, or uniform motion in order to achieve the function of the car adaptive cruise system [27, 28].

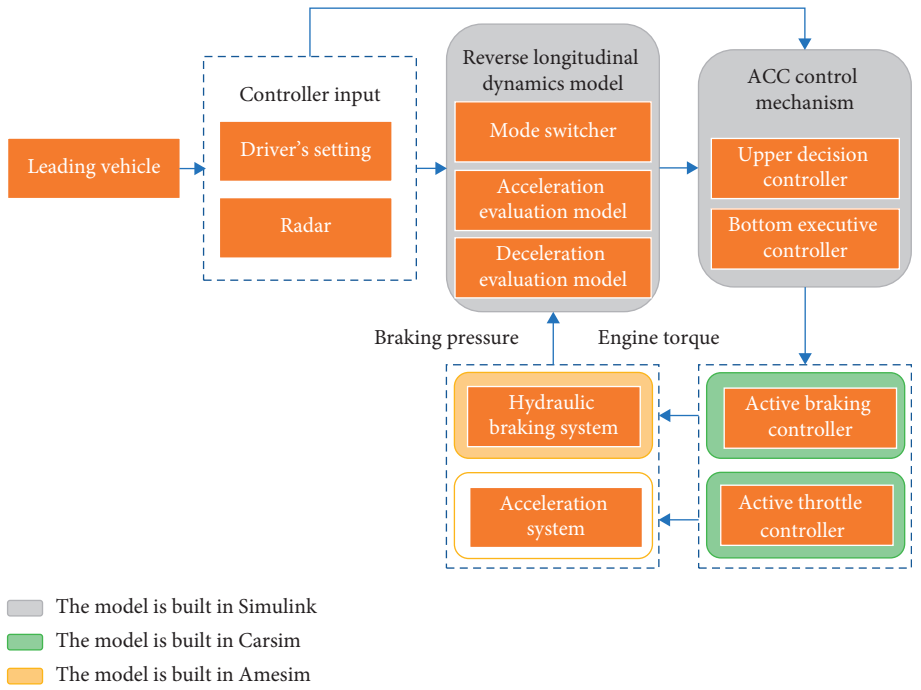

Figure 1: Scheme of the proposed ACC control model.

Table 1: Parameters of the vehicles.

Parameters	Symbol	Value
Sprung mass (kg)	M	1111
Distance between CM and front axle (m)	a	1.04
Distance between CM and rear axle (m)	b	1.56
Air density (kg/m^3)	ρ	1.206
Rolling resistance coefficient	f	0.02
Track (m)	d	1.695
Centroid height (m)	H	0.54
Gear ratio of main gear	i_0	4.1
Transmission gear	N	6
Gear ratio of transmission	i_g	1
Tire rolling radius (m)	r	0.311
Air resistance coefficient	C_D	0.342
Frontal area (m^2)	A	1.6
The efficiency of the drive system	η	0.9

2.2.1. Mode Switch. To the vehicle dynamics system, acceleration and braking are separate movements. When braking, the car should first release the accelerator pedal, using engine drag, wind resistance, and rolling resistance and other ways to brake. If the above action still cannot meet the needs of vehicle deceleration, then depress the brake pedal, applying brake force to increase vehicle deceleration. Besides, taking into account the driving comfort and the reliability of the corresponding parts of the vehicle, the designing process should avoid frequent switching between acceleration control and braking control.

It is easy to directly measure the maximum deceleration value a_{max} at different speeds in Carsim software, as shown in Figure 2. In order to improve the driving comfort of the vehicle, the width of the transition area is set on the upper and lower sides of the switching curve, which is generally taken from experience.

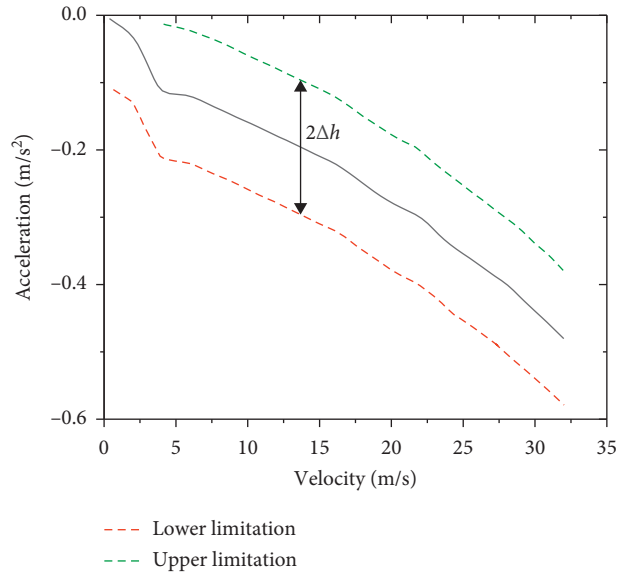

Figure 2: Acceleration control/braking control switching curve.

The expected acceleration of the vehicle is defined as a_{fdes}. According to the switching curve, when $a_{fdes} \geq a_{max}$, the car switches to acceleration control. On the contrary, when $a_{fdes} \leq a_{max}$, the car switches to braking control.

2.2.2. Acceleration Control. If the vehicle switches to acceleration control mode, it is necessary to do as the expected acceleration requires. The expected torque is calculated from

the expected acceleration, and then the desired throttle opening can be checked through the engine mapping.

Without considering the conversion quality of rotating parts, the longitudinal dynamic analysis of the vehicle is analyzed and the vehicle longitudinal dynamics model is as follows:

$$ma_{\text{fdes}} = F_{\text{t}} - F_{\text{xb}} - \sum F(v),$$
$$\sum F(v) = \frac{1}{2}C_{\text{D}}A\rho v^2 + mgf, \tag{1}$$

where a_{fdes} is the expected acceleration, m is the vehicle mass, F_{t} is the driving force, F_{xb} is the braking force, $\sum F(v)$ is the sum of the resistances, C_{D} is the air resistance coefficient, A is the frontal area, ρ is the air density, v is the car speed, g is the gravitational acceleration, and f is the rolling resistance coefficient.

Regardless of the elastic deformation of the transmission system, the driving force can be calculated as follows:

$$F_{\text{t}} = \frac{\eta\tau(\omega_{\text{t}}/\omega_{\text{e}})i_{\text{g}}i_0}{r}T_{\text{e}} = K_{\text{d}}T_{\text{e}}, \tag{2}$$

where η is the mechanical efficiency, T_{e} is the engine torque, ω_{t} is the torque converter turbine speed, ω_{e} is the engine speed, i_{g} is the transmission gear ratio, i_0 is the main gear ratio, $\tau(\omega_{\text{t}}/\omega_{\text{e}})$ is a torque converter characteristic function, r is the wheel rolling radius, and K_{d} is a variable that can be observed in real time:

$$K_{\text{d}} = \frac{\eta\tau(\omega_{\text{t}}/\omega_{\text{e}})R_{\text{g}}R_{\text{m}}}{r} = \frac{\eta\tau\left(\left(vR_{\text{g}}R_{\text{m}}\right)/\left(r\omega_{\text{e}}\right)\right)R_{\text{g}}R_{\text{m}}}{r}. \tag{3}$$

When the vehicle is accelerating, $F_{\text{xb}} = 0$. And the expected engine output torque can be obtained according to the transmission gear ratio and speed ratio:

$$T_{\text{des}} = \frac{ma + \sum F(v)}{K_{\text{d}}}. \tag{4}$$

It is easy to get the throttle opening of the engine from the mapping by taking the throttle opening required to output different torques at different speeds. The values are expressed as follows:

$$\alpha_{\text{des}} = f\left(T_{\text{des}}, \omega_{\text{e}}\right). \tag{5}$$

2.2.3. Braking Control. If the car switches to braking control mode, it is necessary to do as the expected deceleration requires. The desired braking force can be calculated according to the desired acceleration, and the braking pressure can be obtained through the braking reverse model [29].

In this case, the engine output torque is terminated, $T_{\text{e}} = 0$; according to equation (2), it can be seen that $F_{\text{t}} = 0$; the vehicle longitudinal force can be shown as

$$ma_{\text{fdes}} = -F_{\text{xb}} - \sum F(v). \tag{6}$$

The braking force and braking pressure can be approximated as a linear relationship as follows:

$$F_{\text{bdes}} = K_{\text{b}}P_{\text{des}}, \tag{7}$$

where K_{b} is a constant.

It is not hard to calculate the braking pressure from equations (6) and (7):

$$P_{\text{des}} = \frac{\left|-ma_{\text{fdes}} - 0.5C_{\text{D}}A\rho v^2 - mgf\right|}{K_{\text{b}}}. \tag{8}$$

2.3. Active Braking Hydraulic System Model. The expected acceleration got from upper-level decision controller is transformed by the inverse vertical dynamic model into the desired braking pressure or desired throttle opening to the underlying accelerator and brake actuator. Active braking objective is archived by controlling the plunger pump and valves to start or stop to achieve the object hydraulic oil pressure, thereby controlling the brake calipers.

2.3.1. Designing of the Active Braking Principle. The simplified hydraulic structure of active braking system is shown in Figure 3. The working principle is as follows. If the system switches into the active braking mode, there are three active modes: booster, packing, and decompression. When pressure increases, high-pressure directional valve 6 and directional valve 5 are opened and the pump motor is started. Brake fluid flows through high-pressure valve 6 and motor pump and then through the inlet valve 12 into the wheel cylinder, then pushing the piston of wheel cylinder to slow down the wheel rotate speed. When braking force reaches a certain intensity, active braking system switches into the pressure hold-on mode, directional valve 5 is opened, pump motor and high-pressure valve 6 are closed, and wheel cylinder pressure keeps constant at this state. When pressure decreases, the high-pressure valve 6 is opened, directional valve 5 and the motor are closed, and the braking fluid flows into the low-pressure accumulator 9, increasing the braking fluid storage of the accumulator. In the process of the new pressure increase case, plunger pump 8 works, and the braking fluid flows out of the low-pressure accumulator 9 and then through inlet valve 12 to the wheel cylinder.

2.3.2. Modeling of the Hydraulic Braking System

(1) Accumulator model

The pressure and volume of the accumulator follow the idea gas law. The mathematical model is as follows:

$$P_A V_A^n = P_1 V_1^n = P_2 V_2^n, \tag{9}$$

where P_A and V_A are the inflation pressure and accumulator capacity, respectively, P_1 and P_2 are the highest and the lowest pressure values of the accumulator, and V_1 and V_2 are the highest and the lowest volume values of the accumulator. Considering that the braking process could be seen as

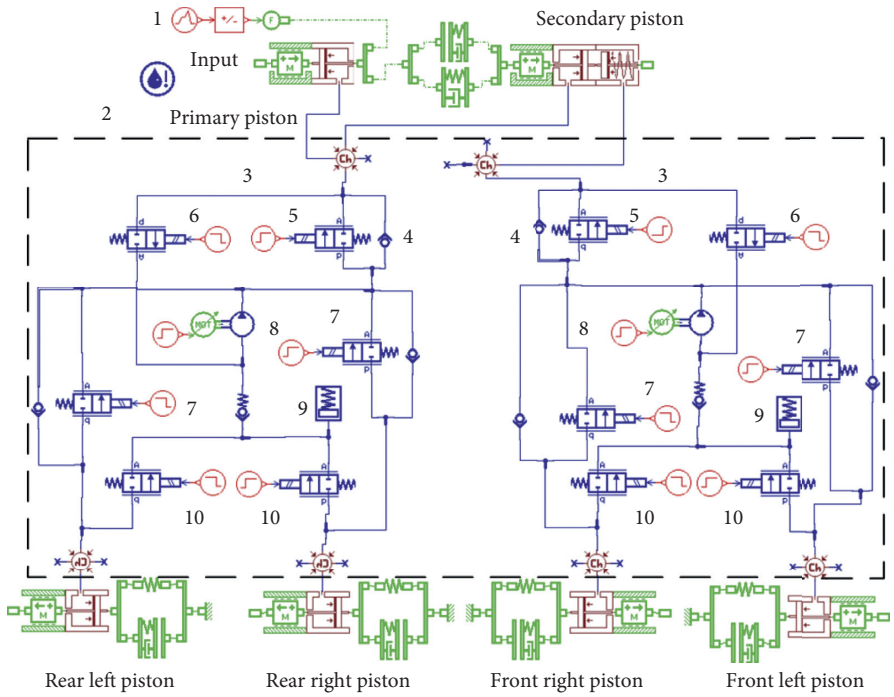

FIGURE 3: Schematic of the active hydraulic braking system. (1) Master cylinder; (2) hydraulic unit; (3) hydraulic circuit; (4) check valve; (5) directional valve; (6) high pressure directional valve; (7) pressure-increasing valve; (8) oil returning pump; (9) low pressure accumulator; (10) pressure-reducing valve.

adiabatic, $n = 1.4$. Apart from these, P_A should meet the requirement that $0.25P_1 < P_A < 0.9P_2$.

(2) Motor pump model

The motor starts to work when the accumulator pressure is below the lower limit and stops when the accumulator pressure reaches the upper limit. The mathematical model is as follows [30]:

$$Q_b = V_c \omega \frac{E}{E[\alpha P_{in} + (1-\alpha)P_{out}]}, \tag{10}$$

(i) where Q_b is the oil pump flow rate, V_c is the pump displacement, ω is the motor speed, P_{out} and P_{in} are the output and input of pump pressure, respectively, E is the bulk modulus of braking fluid, and α is the pump pressure factor.

(3) High-speed switch solenoid switch model

For the on-off action of the solenoid switch that is controlled by the input voltage, there will be a certain delay phenomenon. In addition, inertia of the spool can also cause delay. The mathematical model of the high-speed on-off valve with the second-order delay is as follows:

$$G(s) = \frac{K_1 \omega}{s_2 + 2\xi\omega s + \omega^2}, \tag{11}$$

where K_1 is the current gain, ω is the valve frequency, and ξ is the equivalent damping ratio of the valve.

(4) Restrictor model

The restrictor controls the flow rate by the order of system pressure, and the mathematical model is as follows:

$$q = a \tanh\left(\frac{2\chi\sqrt{((2\Delta p)/\rho)}}{\nu \mathrm{Re}}\right)_{q\max}, \tag{12}$$

where q is the hydraulic medium flow, A is the effective circulation area of valves, χ is the hydraulic diameter, ρ is the fluid density, Δp is the valve's pressure difference, ν is the sports viscosity, and Re is the critical Reynolds number.

(5) Braking model

The braking model is as follows:

$$m\frac{d^2b}{dt^2} = -PS + C_{eq}\frac{db}{dt} + K_m(b_0 + b), \tag{13}$$

$$bS = \int_0^t Q dt,$$

where m is the brake caliper mass, b is the brake caliper displacement, P is the hydraulic cylinder braking pressure, C_{eq} is the equivalent damping, K_m is the spring stiffness, x_0 is the spring initial position, and S is the area of hydraulic cylinder cross section.

3. Control Algorithms

Due to the complex conditions of the vehicle following, the former researches have shown that the ACC system should

both control the vehicle speed and adapt to external interference such as the leading vehicle's velocity [31, 32]. Independent hierarchical control method is used in the proposed ACC model. And the control method is divided into the upper controller (decision-making controller) module and the bottom controller (underlying executive module controller).

The upper controller determines the expected acceleration a_{fdes} based on the driving information provided by the sensors and the driver's settings at this time. Based on the output from the upper controller, the bottom controller makes the vehicle dynamics system to achieve the desired acceleration.

3.1. Upper Controller Design

3.1.1. Establishment of the Follower Model. Car-following model is built based on the driver desired distance and the vehicle dynamic characteristic. Equation (14) describes the driver desired distance [33], and equation (15) shows the relationship of the vehicle dynamic:

$$d_{\text{des}} = T_{\text{h}} v_{\text{f}} + d_0, \tag{14}$$

where d_{des} is the expect distance, T_{h} is the time headway, v_{f} is the velocity of the following vehicle, and d_0 is the minimum safe distance when the two vehicles stop.

It is clear that the distance error and the velocity difference can be as follows:

$$\begin{cases} \Delta d = d_{\text{des}} - d, \\ \Delta v = v_{\text{l}} - v_{\text{f}}, \end{cases} \tag{15}$$

where d is the factual distance, Δd is the distance error, v_{l} is the velocity of the leading vehicle, and Δv is the velocity difference.

A simulation system is built to analyze the vehicle dynamic relationship. The frequency response method is adopted to identify the system input and output characteristics, and finally the transfer function is obtained as equation (18):

$$a_{\text{f}} = \frac{K}{Ts + 1} a_{\text{fdes}}, \tag{16}$$

where K is the gain and T is the time delay.

Combining equations (16)–(19), the car-following model can be as follows:

$$\dot{x} = A' x + B' u + G' v, \tag{17}$$

where $x = [\Delta d \, \Delta v \, a_{\text{f}}]^T$, $u = a_{\text{fdes}}$, $\lambda = a_{\text{p}}$, $A' = \begin{bmatrix} 0 & 1 & -T_{\text{h}} \\ 0 & 0 & -1 \\ 0 & 0 & -(1/T) \end{bmatrix}$, $B' = \begin{bmatrix} 0 \\ 0 \\ K/T \end{bmatrix}$, and $G' = \begin{bmatrix} 0 & 1 & 0 \end{bmatrix}^T$.

x is the system status variable; u is the system input; λ is the disturbance of the input, which is the preceding vehicle's acceleration a_{p} here; A', B', and G' are the coefficient matrix of the input.

3.1.2. Performance Index Design

(1) Following performance index

The ACC system needs to control the vehicle following the leading vehicle steadily, and the following performance is manifested in the performance index of speed and the safety index [34–36].

The square sum of the speed error $\Delta v(k)$ and the distance error $\Delta d(k)$ is taken as the following performance index:

$$l_{\text{t}}(k) = w_{\Delta d} (\Delta d(k))^2 + w_{\Delta v} (\Delta v(k))^2, \tag{18}$$

where $\Delta d(k) = s_{\text{f}}(k) - s_{\text{l}}(k) - d_{\text{des}}(v_{\text{l}}(k))$, $\Delta v(k) = v_{\text{h}}(k) - v_{\text{f}}(k)$,$w_{\Delta d}$ and $w_{\Delta v}$ are the distance error weight and speed error weight, s_f is the displacement of the front car, and s_{h} is the distance of the car traveled.

The following performance index in the forecast time domain is as follows:

$$L_{\text{t}}(k) = \sum_{P}^{k=1} l_{\text{t}}(k) . \tag{19}$$

(2) Safety index

The vehicle should keep a safe distance to avoid collision. Meanwhile, the distance between the two vehicles should avoid being too large to avoid accidental vehicle insertion. The vehicle should also keep an appropriate speed difference to ensure safety and to increase traffic efficiency. And the velocity error between two vehicles should not be too large. The optimization problem is solved subject to desired intervehicle distance and acceleration limitation, which are incorporated as constraints. Therefore, the constraints of the vehicle distance error and speed error are as follows:

$$\begin{cases} 0 \le \Delta d(k) \le \Delta d_{\max}, \\ \Delta v_{\min} \le \Delta v(k) \le \Delta v_{\max}. \end{cases} \tag{20}$$

(3) System prediction optimization

Based on the index functions and constraints established before, the integrated index for the optimization problem is established as follows:

$$L = \sum_{i=1}^{P} \| \Delta d(k+i+1 \mid k) \|^2_{w_{\Delta d}} + \sum_{i=1}^{P} \| \Delta v(k+i+1 \mid k) \|^2_{w_{\Delta v}}, \tag{21}$$

where P is the length of the predictive sample time.

System constraints are as follows:

$$\begin{cases} x_{\min} \le x(k+i \mid k) \le x_{\max}, \\ y_{\min} \le y(k+i \mid k) \le y_{\max}, \end{cases} \quad i = 0 : P-1. \tag{22}$$

From the above analysis, the objective optimization problem of the system can be described as follows:

$$\min_{i=0:\ P-1} L, \tag{23}$$

subject to

$$\begin{cases} 0 \le \Delta d(k) \le \Delta d_{\max}, \\ \Delta v_{\min} \le \Delta v(k) \le \Delta v_{\max}, \\ x_{\min} \le x(k+i \mid k) \le x_{\max}, \\ y_{\min} \le y(k+i \mid k) \le y_{\max}. \end{cases} \tag{24}$$

3.2. Bottom Controller Design. The bottom controller is the system that ensures the vehicle response is constant with the expected value calculated by the upper controller as much as possible. The desired acceleration from the upper controller is translated into the desired braking pressure or throttle opening to the braking controller and the throttle controller via the inverse longitudinal braking model.

3.2.1. Throttle Controller. The PID algorithm is adopted in the throttle controller to ensure the system is working in robust and reliable condition. The algorithm takes the linear combination of the error's proportion (P), integral (I), and differential (D) as control variables and controlling object.

The PID control law is as follows:

$$\Delta y = K_{\mathrm{p}}\left[\varepsilon + \frac{1}{T_{\mathrm{I}}}\int_0^t \varepsilon \mathrm{d}t + T_{\mathrm{D}}\frac{\mathrm{d}\varepsilon}{\mathrm{d}t}\right], \tag{25}$$

where ε is the difference between the expected acceleration a_{des} and the actual car acceleration a, K_{p} is the proportional gain, T_{I} is the integration time constant, and T_{D} is the derivative time constant.

The conversion to transfer function is as follows:

$$(s) = \frac{U(s)}{E(s)} = K_{\mathrm{p}}\left(1 + \frac{1}{T_{\mathrm{I}}s} + T_{\mathrm{D}}s\right). \tag{26}$$

3.2.2. Braking Controller. The purpose of the braking pressure controller is to make the real braking pressure and the expected as close as possible so as to follow up the desired acceleration. Due to inertial links (mechanical system inertia, electrical system inertia, and control system inertia) of the active braking control system, real-time control value cannot act on the control system timely. Even if the parameters of the classical discrete PID algorithm are optimized, the control result still has serious lag and overshoot, which cannot meet the control requirements. The ideas for solving these problems will be given in the next paragraph.

By using proportional feedback control, it is easy to double the interference noise in feedback acceleration, which is not conducive to the stability. Feedback control structure is used to make the actual pressure follow the target pressure. And the feedforward control structure is used to improve the controller execution response to recuperate the time lag of the feedback controller. The cooperation of the feedback and feedforward controller is used to eliminate the static error and improve the accuracy of acceleration control.

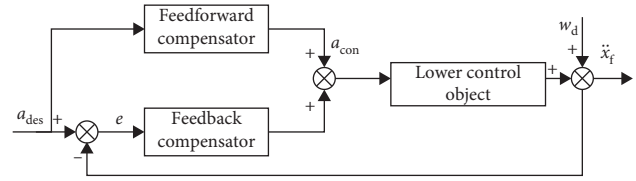

Figure 4: Structure of the braking controller.

Table 2: Duty ratio of high-pressure valve and directional valve under different pressure differences.

X (MPa)	−6	−4	−3	−2	−1	−0.5	−0.3	−0.1	
Y1 (%)	100	40	35	30	25	20	15	10	
Y2 (%)	0	0	0	0	0	0	0	0	
X (MPa)	0	0.1	0.3	0.5	1	2	3	4	6
Y1 (%)	0	0	0	0	0	0	0	0	0
Y2 (%)	0	10	20	20	25	30	40	40	100

The overall structure of the braking controller is shown in Figure 4.

Feedforward compensator uses the look-up table method. According to the pressure difference between the actual pressure and the ideal pressure of the hydraulic cylinder, the system controls the duty cycle signal of the increasing and reducing valve so as to control the pressure change rate of the hydraulic cylinder, precisely controlling the hydraulic cylinder pressure.

When the pressure difference is active, the system will select a larger duty cycle in order to quickly increase or reduce hydraulic cylinder pressure. When the pressure difference is positive, the system will choose a smaller duty cycle to accurately track the ideal pressure, and to improve the wheel pressure accuracy and robustness [37, 38], specifically as listed in Table 2, where X is the pressure difference, Y1 is the valve duty signal of the booster valve, and Y2 is the duty cycle of the valve control signal of the pressure reducing valve.

Similar to the throttle controller, the PID algorithm is used in the braking controller. The difference between the expected braking pressure and the actual braking pressure is taken as the target control variable. From the design process, one can conclude that the designs of the feedforward compensator and the feedback compensator do not affect each other and can be performed independently.

4. Simulation and Discussion

A collaborative simulation model is built by Matlab/Simulink, Carsim, and Amesim to validate the proposed algorithm. The simulation parameters and restrictions are defined, as shown in Table 3.

Simulation conditions are as follows: at 0–15 s, the leading vehicle drives at 20 m/s; at 15–25 s, the leading vehicle accelerates to 30 m/s with acceleration 1 m/s^2; at 25–35 s, the leading vehicle drives at 30 m/s; at 35–42 s, the leading vehicle slows down to 18 m/s with deceleration −1.7 m/s^2. The initial distance between two vehicles is 50 m, and the initial speed of the follower vehicle is 25 m/s. The simulation results are shown in Figures 5–8. The follow process includes 3 stages, shown as follows.

Table 3: The simulation parameters.

Items	t_s (s)	t_h (s)	τ (s)	d_0 (m)	d_c (m)	$v_{\min}$ (m/s)	$v_{\max}$ (m/s)
Value	0.2	1.5	0.7	7	5	0	36
Items	$a_{u\min}$ (m/s^2)	$a_{u\max}$ (m/s^2)	R	N	P	R	
Value	−3	2	1	5	10	diag{2, 10, 0}	

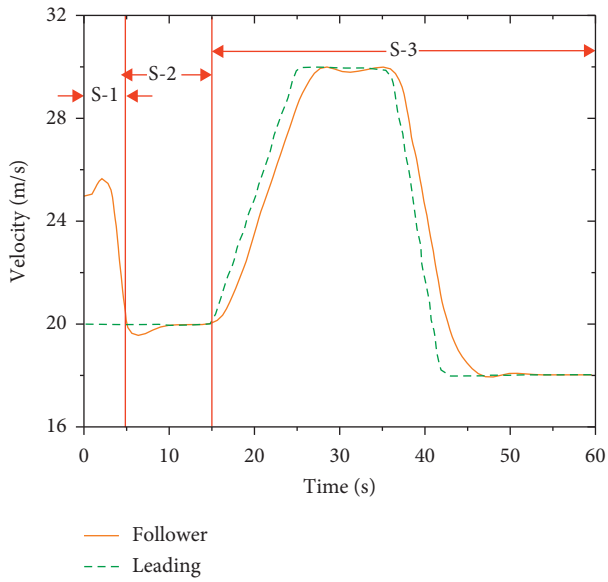

Figure 5: The vehicle velocity of the two vehicles.

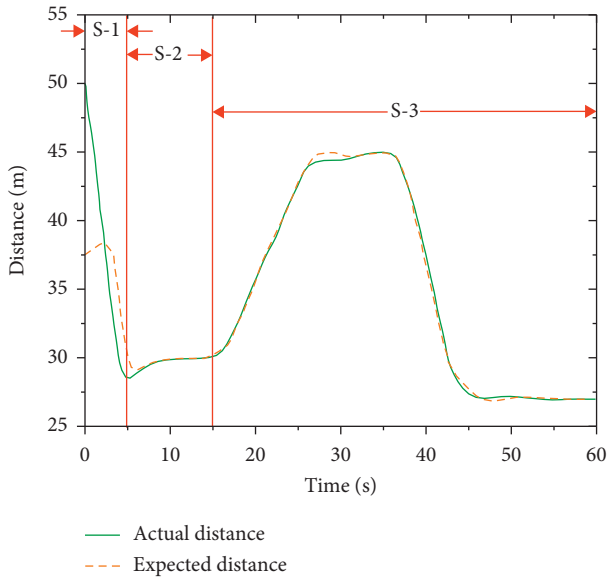

Figure 6: Distance between the two vehicles.

4.1. S-1 Follow Distance Adjustment. During the time 0 – 5 s, the actual distance between the two vehicles is greater than the desired distance; the system judges the condition is safe. The upper controller instructs the bottom controller to accelerate to shorten the distance to improve the traffic efficiency. The braking controller is on the standby mode, and the throttle is in a small opening. As the velocity increases, the expected distance also increases.

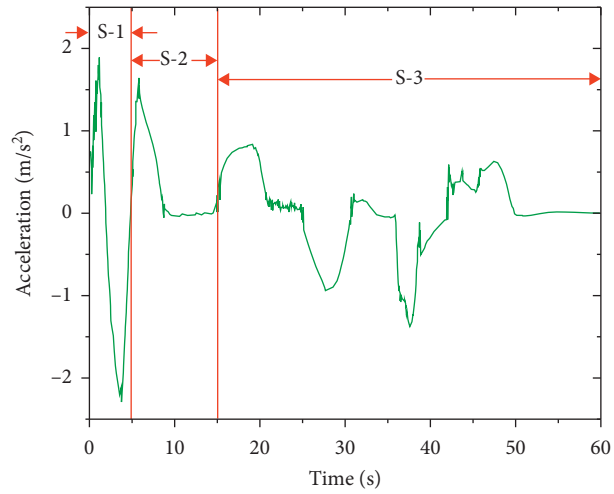

Figure 7: Acceleration of the follower vehicle.

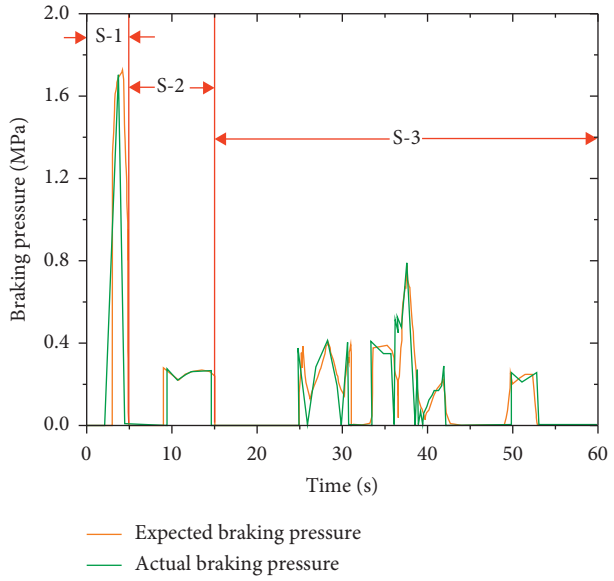

Figure 8: Braking pressure of the follower vehicle.

4.2. S-2 Follow Velocity Adjustment. As the velocity of the follower vehicle increases, the expected distance increases also. The actual distance is shortened as the velocity difference increases; the system judges the condition is in danger. The upper controller instructs the bottom controller to decelerate to lengthen the distance to improve the safety. The throttle controller is on the standby mode; the braking controller opens valves 5 and 6 and starts the brake pump (Figure 3); and the braking pressure is increased. And then, the vehicle deceleration increases, and the velocity of the follower vehicle decreases near the velocity of the leading vehicle.

4.3. S-3 Follow with the Leading Vehicle. As the leading vehicle accelerates during 15–25 s and decelerates during 35–42 s, the follower vehicle changes the throttle opening and braking pressure, keeping the desired distance and speed. As can be seen from Figure 7, although the acceleration of the vehicle has slight fluctuation, the acceleration falls in a narrow range of −3 to 2 m/s^2, which ensures the ride comfort. As can be seen in Figure 8, the target pressure follows the change of the desired acceleration response quickly and steadily with less hysteresis.

To illustrate purposes and evaluate results conveniently, a comparison with a state-of-the-art ACC used in the automotive industry research is analyzed [39]. In this paper, the safety and comfort are evaluated and provided directly. The full declaration method is used in the mode which presents detailed simulation results for one considered scenario. The results show that the velocity of the leading vehicle accelerates from 10 m/s–15 m/s and the acceleration of follower vehicle falls in a width range of −10 − 5 m/s^2. The jerk caused by application of full braking results in uncomfortable driving.

By comparison, the proposed strategy results show that the acceleration of the vehicle has slight fluctuation and fast response, which implies comfortable driving without jerky maneuvers. The ability of keeping intervehicle distance as close as possible to safe distance shows good tracking performance. In this way, both safety and comfort are achieved by utilizing the proposed model based on optimization of active braking strategy.

5. Conclusions

This research is aimed at proposing an ACC strategy considering the safety and comfort based on the active braking where the system hysteresis problem is included. For this purpose, vehicle dynamics model, vehicle reverse longitudinal dynamics model, and active hydraulic braking system model are proposed. And the models are simulated in Carsim, MATLAB/Simulink, and Amesim collaboratively. The control algorithm is proposed and optimized to improve the ride comfort. From the results, it can be seen that the velocity and distance values are preserved in the specified comfortable range although the vehicle velocity changes obviously:

(1) The control algorithm based on the model predictive control algorithm can be optimized by considering the multivariable constraints simultaneously; that is to say, the cruise-following control safety can be ensured and the ride comfort can be satisfied.

(2) The proposed algorithm is evaluated by comparison with using full deceleration simulation, and it shows active performance on position and velocity tracking. Thus, we can conclude that the proposed approach guarantees safety and comfort for ACC-equipped vehicles in low velocity conditions.

This study only focuses on the occupant kinematics during the pre-crash period; the occupant kinematics and injury indexes within the in-crash phase of such typical scenario require subsequent study.

Data Availability

All data included in this study are available upon request to the corresponding author.

Conflicts of Interest

The authors declare no conflicts of interest.

Acknowledgments

This research was funded by the National Natural Science Foundation of China under Grant nos. 51775178, 51875049, and 51705035 and Hunan Science Foundation for Distinguished Young Scholars of China under Grant no. 2019JJ20017.

References

[1] L. Hu, J. Ou, J. Huang, Y. Chen, and D. Cao, "A review of research on traffic conflicts based on intelligent vehicles," *IEEE Access*, vol. 8, pp. 24471–24483, 2020.

[2] L. Hu, X. Hu, J. Wan, M. Lin, and J. Huang, "The injury epidemiology of adult riders in vehicle-two-wheeler crashes in China, Ningbo, 2011-2015," *Journal of Safety Research*, vol. 72, pp. 21–28, 2020.

[3] Y. Peng, C. Fan, L. Hu et al., "Tunnel driving occupational environment and hearing loss in train drivers in China," *Occupational and Environmental Medicine*, vol. 76, no. 2, pp. 97–104, 2019.

[4] R. Rajamani, *Adaptive Cruise Control. Vehicle Dynamics and Control*, pp. 141–170, Springer US, Boston, MA, USA, 2012.

[5] A. Weißmann, D. Görges, and X. Lin, "Energy-optimal adaptive cruise control combining model predictive control and dynamic programming," *Control Engineering Practice*, vol. 72, pp. 125–137, 2018.

[6] F. Schrödel, P. Herrmann, and N. Schwarz, "An improved multi-object adaptive cruise control approach," *IFAC-PapersOnLine*, vol. 52, no. 8, pp. 176–181, 2019.

[7] Y. He, B. Ciuffo, Q. Zhou et al., "Adaptive cruise control strategies implemented on experimental vehicles: a review," *IFAC-PapersOnLine*, vol. 52, no. 5, pp. 21–27, 2019.

[8] M. Li, Y. Chen, and C.-C. Lim, "Stability analysis of complex Network control system with dynamical topology and delays," *IEEE Transactions on Systems, Man, and Cybernetics: Systems*, pp. 1–10, 2020.

[9] L. Yang, Y. Chen, Z. Liu, K. Chen, and Z. Zhang, "Adaptive fuzzy control for teleoperation system with uncertain kinematics and dynamics," *International Journal of Control, Automation and Systems*, vol. 17, no. 5, pp. 1158–1166, 2019.

[10] B. Guo and Y. Chen, "Robust adaptive fault-tolerant control of four-wheel independently actuated electric vehicles," *IEEE Transactions on Industrial Informatics*, vol. 16, no. 5, pp. 2882–2894, 2018.

[11] B. Goñi-Ros, W. J. Schakel, A. E. Papacharalampous et al., "Using advanced adaptive cruise control systems to reduce congestion at sags: an evaluation based on microscopic traffic simulation," *Transportation Research Part C: Emerging Technologies*, vol. 102, pp. 411–426, 2019.

[12] J. Zhan, "Setup of vehicle longitudinal dynamic model for adaptive cruise control," *Journal of Jilin University (Engineering)*, vol. 36, no. 2, pp. 157–160, 2006.

[13] S. Huang and W. Ren, "Autonomous intelligent cruise control with actuator delays," *Journal of Intelligent and Robotic Systems*, vol. 23, no. 1, pp. 27–43, 1998.

[14] A. S. A. Rachman, A. F. Idriz, S. Li, and S. Baldi, "Real-time performance and safety validation of an integrated vehicle dynamic control strategy," *IFAC-PapersOnLine*, vol. 50, no. 1, pp. 13854–13859, 2017.

[15] J. E. Naranjo, C. Gonzalez, R. Garcia, and T. DePedro, "ACC+Stop&Go maneuvers with throttle and brake fuzzy control," *IEEE Transactions on Intelligent Transportation Systems*, vol. 7, no. 2, pp. 213–225, 2006.

[16] P. Shakouri, A. Ordys, D. S. Laila, and M. Askari, "Adaptive cruise control system: comparing gain-scheduling PI and LQ controllers," *IFAC Proceedings Volumes*, vol. 44, no. 1, pp. 12964–12969, 2011.

[17] P. Ioannou, Z. Xu, S. Eckert, D. Clemons, and T. Sieja, "Intelligent cruise control: theory and experiment," in *Proceedings of 32nd IEEE Conference on Decision and Control*, pp. 1885–1890, San Antonio, TX, USA, December 1993.

[18] S. Kitazono and H. Ohmori, "Semi-Autonomous adaptive cruise control in mixed traffic," Proceedings of 2006 SICE-CASE International Joint Conferencepp. 3240–3245, Busan, South Korea, October 2006.

[19] M. H. Lee, H. G. Park, S. H. Lee, K. S. Yoon, and K. S. Lee, "An adaptive cruise control system for autonomous vehicles," *International Journal of Precision Engineering and Manufacturing*, vol. 14, no. 3, pp. 373–380, 2013.

[20] X. Wu, G. Qin, H. Yu, S. Gao, L. Liu, and Y. Xue, "Using improved chaotic ant swarm to tune PID controller on cooperative adaptive cruise control," *Optik*, vol. 127, no. 6, pp. 3445–3450, 2016.

[21] N. C. Basjaruddin, K. Kuspriyanto, D. Saefudin et al., "Developing adaptive cruise control based on fuzzy logic using hardware simulation," *International Journal of Electrical & Computer Engineering*, vol. 4, no. 6, 2014.

[22] G. Prabhakar, S. Selvaperumal, and P. N. Pugazhenthi, "Fuzzy PD plus I control-based adaptive cruise control system in simulation and real-time environment," *IETE Journal of Research*, vol. 65, no. 1, pp. 69–79, 2019.

[23] R. Rizvi, S. Kalra, C. Gosalia et al., "Fuzzy Adaptive Cruise Control system with speed sign detection capability," in *Proceedings of 2014 IEEE International Conference on Fuzzy Systems*, pp. 968–976, IEEE, Beijing, China, July 2014.

[24] B. Ganji, A. Z. Kouzani, S. Y. Khoo, and M. Shams-Zahraei, "Adaptive cruise control of a HEV using sliding mode control," *Expert Systems with Applications*, vol. 41, no. 2, pp. 607–615, 2014.

[25] L. Hu, Y. Zhong, W. Hao et al., "Optimal route algorithm considering traffic light and energy consumption," *IEEE Access*, vol. 6, pp. 59695–59704, 2018.

[26] K. Gao, F. Han, P. Dong, N. Xiong, and R. Du, "Connected vehicle as a mobile sensor for real time queue length at signalized intersections," *Sensors*, vol. 19, no. 9, p. 2059, 2019.

[27] D. Hou, *Study on Vehicle Forward Collision Avoidance System*, Tsinghua University, Beijing, China, 2004.

[28] Y. Liu, J. Che, and C. Cao, "Advanced autonomous underwater vehicles attitude control with L 1 backstepping adaptive control strategy," *Sensors*, vol. 19, no. 22, p. 4848, 2019.

[29] H. Zheng and M. Zhao, "Development a HIL test bench for electrically controlled steering system," Proceedings of SAE Technical Paper Series, SAE International, April 2016.

[30] X. Qi J. Song et al., "Modeling and analysis of vehicle ESP hydraulic control device using AMESim," *Machine Tools and Hydraulic*, vol. 8, pp. 115-116, 2005.

[31] S. Moon, I. Moon, and K. Yi, "Design, tuning, and evaluation of a full-range adaptive cruise control system with collision avoidance," *Control Engineering Practice*, vol. 17, no. 4, pp. 442–455, 2009.

[32] D. H. Han, K. S. Yi, J. K Lee, B. S. Kim, and S. Yi, "Design and evaluation of inteligent vehicle cruise control systems using a vehicle simulator," *International Journal of Automotive Technology*, vol. 7, no. 3, pp. 377–383, 2006.

[33] D. Yanakiev and I. Kanellakopoulos, "Longitudinal control of heavy-duty vehicles for automated highway systems," Proceedings of the 1995 American Control Conference, Seattle, WA, USA, June 1995.

[34] M. Guocheng, *Research on the Adaptive Cruise Control Tracking System Applied for Motor Vehicle*, Beijing Institute of Technology, Beijing, China, 2014.

[35] Z. Zhang, D. Luo, Y. Rasim et al., "A vehicle active safety model: vehicle speed control based on driver vigilance detection using wearable EEG and sparse representation," *Sensors*, vol. 16, no. 2, p. 242, 2016.

[36] R. Du, G. Qiu, K. Gao, L. Hu, and L. Liu, "Abnormal road surface recognition based on smartphone acceleration sensor," *Sensors*, vol. 20, no. 2, p. 451, 2020.

[37] L. Hu, X. Hu, Y. Che et al., "Reliable state of charge estimation of battery packs using fuzzy adaptive federated filtering," *Applied Energy*, vol. 262, 2020.

[38] Z. Zhang, L. Zhang, L. Hu, C. Huang et al., "Active cell balancing of lithium-ion battery pack based on average state of charge," *International Journal of Energy Research*, vol. 44, no. 4, pp. 2535–2548, 2020.

[39] S. Magdici and M. Althoff, "Adaptive cruise control with safety guarantees for autonomous vehicles," *IFAC-PapersOnLine*, vol. 50, no. 1, pp. 5774–5781, 2017.